

[SSC19-WKV-04]

Solar System Exploration Sciences by EQUULEUS on SLS EM-1 and Science Instruments Development Status

Satoshi Ikari, Masahiro Fujiwara, Hirotaka Kondo, Shuhei Matsushita, Ichiro Yoshikawa,
Kazuo Yoshioka, Reina Hikida, Yosuke Kawabata, Shintaro Nakajima, Ryu Funase
The University of Tokyo
7-3-1 Hongo, Bunkyo-ku, Tokyo 113-8656, Japan; +81-3-5841-6608
ikari@space.t.u-tokyo.ac.jp

Masaki Kuwabara, Hajime Yano, Kota Miyoshi, Tatsuaki Hashimoto
JAXA/Institute of Space and Astronautical Science, Japan

Shinsuke Abe, Ryota Fuse, Yosuke Masuda, Shosaku Harima
Nihon University, Japan

Masahisa Yanagisawa, Kenji Yamamoto, Ryuji Shimada
The University of Electro-Communications, Japan

Takayuki Hirai
Chiba Institute of Technology, Japan

Haruki Nakano, Kosuke Kando, Kazuyoshi Arai
Hosei University, Japan

Masayuki Fujii
FAM Science, Japan

David Veysset, Yuchen Sun, Steven Kooi, Keith Nelson
Massachusetts Institute of Technology, the United States

ABSTRACT

EQUULEUS is a spacecraft to explore the cislunar region including the Earth-Moon Lagrange point L2 (EML2) and will be launched by NASA's SLS EM-1 rocket. Although the size of EQUULEUS is only 6U, the spacecraft carries three different science instruments. By using these instruments, the spacecraft will demonstrate three missions for solar system exploration science during and after the flight to EML2; imaging of the plasmasphere around the earth, observation of space dust flux in the cislunar region, and observation of lunar impact flashes at the far side of the moon. The developments and verifications of the flight models of these science instruments were completed by the end of 2018, and we started flight model integration and testing. This paper introduces the details of the scientific objectives, design results and development statuses of the instruments. In addition, results of the integration and pre-flight tests are also described.

INTRODUCTION

In 2014, as the first interplanetary micro-spacecraft, "PROCYON" has been developed and launched by the University of Tokyo (UT) and JAXA. The technological and scientific missions of the spacecraft have been successfully demonstrated.^{1,2,3} After that, the first interplanetary CubeSats "MarCO-A and -B" developed by NASA/JPL have been launched together with "InSight" in 2018, and successfully supported the communication between InSight and the ground station

during the EDL (Entry, Descent, and Landing) phase.⁴ The breakthrough of these two interplanetary nano- and micro-spacecraft missions opened the door for a low-cost and effective deep space exploration, and many small deep space missions are being planned all over the world.

To realize advanced interplanetary nano-spacecraft missions, thirteen CubeSats will be launched as secondary payloads onboard the first flight of Space Launch System (SLS EM-1). SLS EM-1 will provide

opportunity to launch into a lunar flyby trajectory for the thirteen 6U CubeSats. As one of the secondary payloads, JAXA and UT will provide a 6U CubeSat named EQUULEUS (EQUilibriUm Lunar-Earth point 6U Spacecraft) to explore the cislunar region including the Earth-Moon Lagrange point L2 (EML2).

This paper describes the details of the scientific missions of EQUULEUS. Firstly, we introduce the overview of EQUULEUS mission. Next, the science objective, the design result of the flight model, and the current development status of the three scientific payloads installed on the spacecraft are described. Finally, the integration and test results of the whole spacecraft are summarized.

OVERVIEW OF EQUULEUS

Figure 1 illustrates the external view of EQUULEUS. EQUULEUS is a 6U (10cm * 20cm * 30cm) CubeSat with four strings solar array paddles, and its weight is about 12 kg. The primary mission objective of EQUULEUS is a demonstration of trajectory control to reach to the EML2. To realize the trajectory control, the spacecraft has basic capabilities required for deep space probes like a three-axis attitude stabilization, a deep space communication and navigation, and an orbit control by using thrusters. Details of these bus systems are described in the conference papers in the References. 5-11

The spacecraft will also demonstrate three scientific missions for solar system exploration during and after the flight to EML2; imaging of the plasmasphere around the earth, observation of space dust flux in the cislunar region, and observation of lunar impact flashes (LIFs) at the far side of the moon. For the three scientific missions, EQUULEUS has three different scientific instruments named PHOENIX, CLOTH, and DELPHINUS. The details of these instruments are described in following sections.

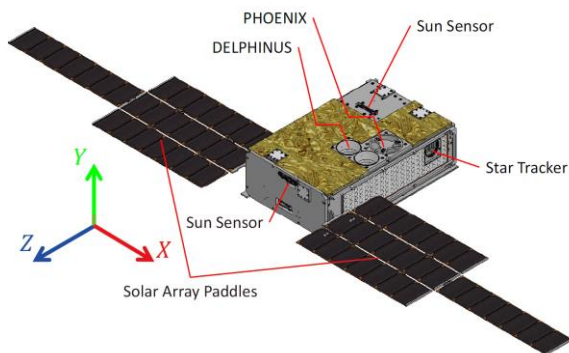


Figure 1: External view of EQUULEUS⁵

PHOENIX: PLASMASPHERE TELESCOPE

Science Objective

PHOENIX (Plasmaspheric Helium ion Observation by Enhanced New Imager in eXtreme ultraviolet) is a telescope to observe extreme ultraviolet emission from He⁺ in the earth's plasmasphere. The primary science objective of this telescope is to clarify the physical process governing the terrestrial plasmas of the earth and improve our understanding of the radiation environment around the earth. The second objective is observation of the plasmasphere structure with respect to the magnetic field of the earth to improve the understanding of the evolution of the atmosphere of the earth and earth-like planets. The whole view of the plasmasphere cannot be observed in low earth orbits since the plasmasphere expands over 10-Re radius. Thus, a lunar probe EQUULEUS is a good opportunity to observe the whole view of the large structure. The plasmasphere observation is mainly conducted on the way to the EML2.

Design

PHOENIX is constructed with an optical part, a high-voltage circuit, a mechanical shutter, and a control circuit board. The specifications of PHOENIX are summarized in Table 1, and the flight model of the telescope and the circuit board to control the telescope are shown in Figure 2. The basic method to observe extreme ultraviolet has been verified in the several former space missions.^{12,13,14}

Table 1: Specifications of PHOENIX

Content	Value
Mass and size of telescope	0.48 kg / 70 × 70 × 100 mm
Mass and size of circuit board	0.06 kg / 100 × 100 mm
Power	1.8 W (maximum)
Field of view	11.9×11.9 deg
Spatial resolution	0.085 deg (0.1 Re from the moon orbit)
Count rate	3 count/min/pix/Rayleigh

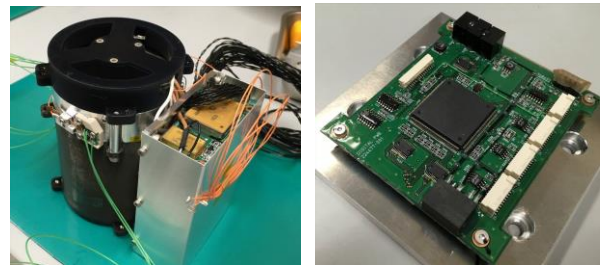


Figure 2: Flight model of PHOENIX (left: Telescope, right: Circuit board)

The optical part consists of a 53-mm diameter primary mirror, a metallic thin filter, and three-stage microchannel plates (MCP). The focal length is 69.4 mm, and spatial resolution is 0.1-Re at the moon orbit. The surface of the primary mirror is coated by Mo/Si to enhance the reflectance of 30.4-nm wavelength (extreme ultraviolet from He⁺) and to eliminate contamination from other wavelengths such as 121.6 nm (H) and 58.4 nm (He). The thin filter additionally eliminates the signal contamination. The MCP device converts the incoming photons into electron clouds, and a high voltage (around 2.5kV) is impressed to generate an electron avalanche and to obtain the sufficient gain. The electron clouds are collected onto the resistive anode with three channels. The position of an incoming photon can be calculated from the relative gain between three corners.

To get a clear image of the plasmasphere by using PHOENIX, an hour integration time is required. EQUULEUS has to stabilize its attitude within 0.08-deg (3-sigma) accuracy during the exposure time. Since an hour stabilization is too long for CubeSats, we divided the exposure time to 10 minutes × 6 shots, and these 6 images will be downlinked and integrated on the ground. For a long and frequent observation of the plasmasphere, EQUULEUS continuously takes images by using PHOENIX during the cruising phase to the EML2. We can totally observe the plasmasphere over four months, and take an image every ten minutes in the minimum period. The main OBC (OnBoard Computer) of EQUULEUS has enough storage for the large amount of image data.

The mechanical shutter is attached to protect the thin filter from overheat by the direct incidence of the solar light. An iris diaphragm mechanism is selected as the shutter system, and the iris is driven by two biometal fibers to open and close the shutter. The shutter also has magnetic sensor to detect whether the shutter is opened or closed. To protect the thin film from sun light, an autonomous shutter closing algorithm is essential. The algorithm implemented on the main OBC detects a failure of the attitude control system, and generates a command to close the shutter.

Development Status

The optics of PHOENIX mentioned above was developed and tuned to reach the required performance. The focus is optimized by modifying the distance between the mirror and the detector with various thickness of shims. For this optimization process, the CCD detector which is attached at the same optical plane as the MCP is used because the MCP is not applicable for the operation outside the vacuum condition. Figure 3 is test image taken by the CCD with

PHOENIX optics. Figure 4 shows the simulated focal length dependency of the radius of the 50% encircled energy (ECE). The final optimization test with flight model is planned to be made in the coming summer.

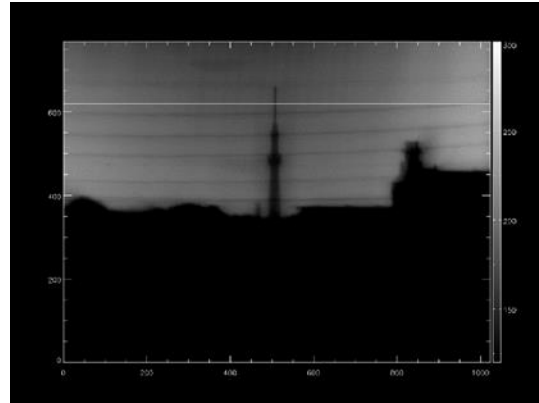


Figure 3: Test image taken by PHOENIX optics and CCD

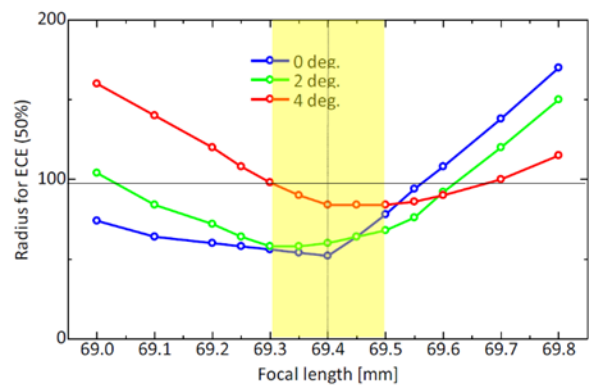


Figure 4: Focal length dependency of the simulated spot size for various incident angles

The robustness of the mechanical shutter during the launch was verified in a unit vibration test. In the prototype model, the shutter has been accidentally opened during the vibration test. After that, to prevent the accidental open of the shutter, the buckle design was changed, and the center of mass was aligned to the geometric center of the shutter by using small counter masses. Then the mechanical robustness was completely verified in the unit vibration test for the flight model. Furthermore, the mechanical shutter open/close driving test was successfully demonstrated hundred times in a vacuum chamber after the vibration test.

CLOTH: DUST DETECTOR

Science Objective

CLOTH (Cis-Lunar Object detector within Thermal insulation) is a dust detector within multi-layered thermal insulator (MLI) to observe micrometeoroids environment in the cislunar region. The primary goal of CLOTH is to provide the first insight of spatial distribution of sub-mm solid objects in the cis-lunar space. It is complementary observation of LIFs by cm-order solid objects. By combining results of both CLOTH and DELPHINUS (described in the next section), we will learn spatial distribution and temporal variation of solid objects in the cis-lunar space, which will benefit Solar System science.

In addition, CLOTH can isolate thermal incidence and emission between the spacecraft interior and space environment, so that we can control the internal temperature of spacecraft. The integrated dust detector with a MLI, which we call “smart MLI”, can efficiently expand the effective area of the sensors in the limited size of CubeSats. The secondary mission is demonstration of the new smart MLI concept. The MLI is easy to use for other satellites and spacecraft which needs MLI for thermal control. Then, all spacecraft can detect impacts of dust for space debris or natural dust monitoring.

Design

CLOTH is constructed with the smart MLI parts, and a control circuit board. The specifications of CLOTH are summarized in Table 2, and the flight model of the two of integrated sensors for the plus Y and the minus Y plane and the circuit board are shown in Figure 5. The sensor design is based on the dust detector named ALADDIN mounted on IKAROS spacecraft.^{15,16}

The detailed architecture of the smart MLI is illustrated in Figure 6. PVDF (PolyVinylidene DiFluoride) piezoelectric films are used for the dust sensor and installed inside the MLI. The total sensitive area is decided to detect one dust larger than 3-um diameter per month in minimum. CLOTH instrument is activated almost all of the flight time of EQUULEUS. During the two years mission life, we expect that we can detect over twenty micrometeoroids around the cislunar region. The signal from the PVDF films is inputted to the circuit board. The board has several analog circuits for signal processing: pre-amplifiers, band-pass filters, rectifiers, and integrators. The integrated signal is analyzed by the digital processing unit on the circuit board, and dust detection flags are sent to the main OBC. When a dust detection flag indicates a dust is detected, the main OBC automatically store the sensor

data around (i.e., future and past) the detected timing to a non-volatile memory.

The remarkable feature of CLOTH compared to the conventional dust detectors is its light weight and large sensor area without any special thermal control. The conventional detectors were developed as a dedicated instrument for science missions, so the ratio of sensor area to instrument mass tends to be low e.g. 1000 cm² at >5 kg. On the other hand, CLOTH achieves about 50 times higher area/mass ratio thanks to our smart MLI concept.¹⁷

The smart MLI was designed not only for the dust detection but also for the passive thermal control of the spacecraft. To satisfy a requirement from thermal design for EQUULEUS mission, the effective absorption α and the effective emissivity ϵ of the MLI both have to be smaller than 0.05. The expected values are worse than common MLIs ($\alpha, \epsilon < 0.01$) because following specific disadvantages for CubeSat thermal isolation was considered. First disadvantage is smaller size of MLIs for CubeSats. Outer edges of the MLI degrade the isolation performance since the thermal connection between face and back side at the edge is too strong. The outer edge length and MLI area ratio of small MLIs becomes larger than large ones. Thus, the isolation performance of the MLIs of CubeSats tends to be worse than that of large satellites. Second disadvantage is strict envelope limited by a dispenser type rocket interface. During the launch, most of the CubeSats are in boxes attached with rockets and should not exceed the envelope constraint. In order to satisfy the constraint, the face and back side of the MLI for EQUULEUS is roughly connected by sewing. The sewing points transfer heat from face to back side, and the thermal isolation performance is degraded. The thermal isolation layers of the smart MLI was designed based on that of PROCYON spacecraft,¹ and several proto types were developed and tested whether the thermal isolation performance satisfies the requirement of the mission.

Table 2: Specifications of CLOTH

Content	Value
Total mass of sensors	0.03kg
Mass and size of circuit board	0.03 kg / 100 × 100 mm
Power	1.0 W (maximum)
Total sensitive area	439cm ²
Detectable dust size	> 4um at > 10 km/s



Figure 5: Flight model of CLOTH (left: Smart MLI, right: Circuit board)

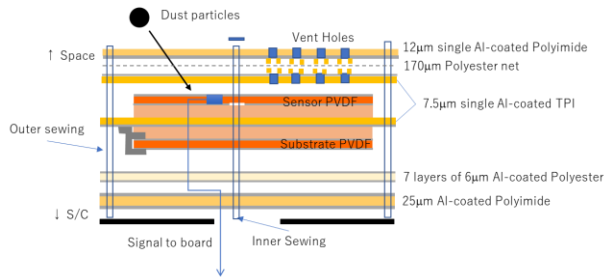


Figure 6: Detail of the dust sensor integrated within MLI

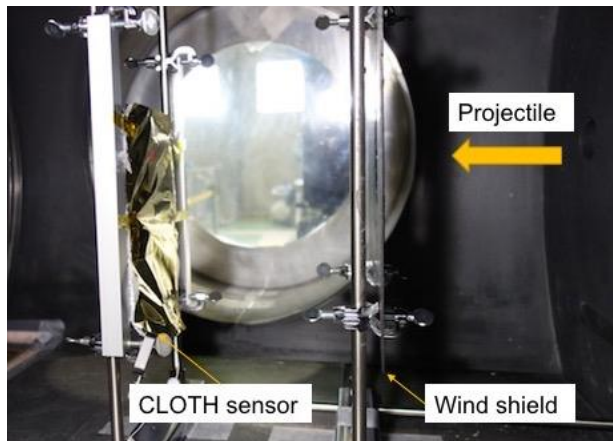


Figure 7: Experiment setup of the hypervelocity impact tests with the light gas gun of JAXA/ISAS.

Development Status

The flight model of CLOTH was already developed as shown in Figure 5. A unit thermal cycle test and a vibration test were successfully finished. Furthermore, in order to verify the capability of dust detection, a high-speed impact test is conducted. Figure 7 shows the experiment setup inside the vacuum chamber at the hypervelocity impact tests with the light gas gun of JAXA/ISAS. We used the test piece of CLOTH sensor which has the same layer configuration made of the

same materials as the flight model of the MLI. The sensor was connected to the flight spare of the circuit board outside the chamber. Micron-sized dust simulant particles (projectile) made of soda-lime glass were accelerated up to 6 km/s mainly with the single shot style.¹⁸ At the projectile impact, the analog signal waveforms generated on the electronics were recorded to the digital storage oscilloscope.

From the signal amplitude analysis and the microscopic observation of impact holes or craters left on the MLI, the dust detection performance of CLOTH was estimated in light of both the penetration threshold of sensor part (the outermost layer of MLI) and the amplification magnitude of electronics part. The final determination of detection performance of the flight model will be finished in the near future though; we here report the current calibration results. A numerical simulator we developed revealed that CLOTH has a capability of detecting a dust particle with $\sim 4 \mu\text{m}$ at the impact velocity of 10 km/s including the amplification magnitude of electronics¹⁹.

According to the thermal vacuum test for the proto type model of EQUULEUS, the thermal isolation performance of the smart MLI was estimated as $\alpha = 0.01$ and $\varepsilon = 0.02$, and these values are better than the expectation mentioned before. It is acceptable to use the MLI as a thermal insulator for EQUULEUS. The analysis verified that the PVDF films to detect dust does not degrade the thermal isolation performance, and the smart MLI concept is applicable for thermal isolation of every spacecraft. However, the proto type MLI has a possibility of EQUULEUS's envelope constraint violation. Hence, we modified the MLI to be thinner for the flight model. The thermal isolation performance may be degraded, but it has enough margin for the thermal design. The final thermal isolation performance was measured in the thermal vacuum test of the flight model of EQUULEUS, and the data will be analyzed soon.

DELPHINUS: LIF TELESCOPE

Science Objective

DELPHINUS (DEtection camera for Lunar impact PHenomena IN 6U Spacecraft) is a telescope system to detect LIFs. A LIF is transient flash generated when a meteoroid strikes to the surface of the moon. In order to investigate size distribution, influx ratio and daily variation of meteoroids around the cislunar region, observations of LIFs are important.

NASA has detected about 430 LIFs in a 10-years ground-based observation.²⁰ However, telescopes on the ground cannot observe the far side of the moon. Hence,

the DELPHINUS will observe the moon from a Halo orbit around the EML2 to detect LIFs including the far side. Since the Halo orbit is approximately 10 times closer to the moon surface than the earth, and there are no light pollution and less influence of earthshine, we can detect darker LIFs by using a smaller telescope. In addition, because a space-based observation is not affected by the weather of the earth, a long-time and continuous observation is possible. Thus, DELPHINUS can detect more and more LIFs than ground observations. Quantitatively, we try to detect over a hundred LIFs in a month²¹. The goal of this observation is not only detecting far side LIFs but also contributing to risk evaluation for future human activities and infrastructures on the lunar surface. There are several similar missions for LIF observation, and DELPHINUS could be the pioneer of these missions.²²

DELPHINUS has also capabilities for asteroid observations such as, TCOs (Temporary Captured Objects) and PHOs (Potentially Hazardous Objects) which will be observed during cruising phase to the EML2.

Design

DELPHINUS is constructed by two cameras and an image processing circuit board. The specifications of DELPHINUS are summarized in Table 3, and the flight model of the telescope and the image processing board are shown in Figure 8. To detect over a hundred LIFs per month, the detectable magnitude is decided as darker than 4.0 Vmag (visual magnitude) with 1/60 second exposure time, and the optical system (i.e. lens and detector) is designed to satisfy the requirement. The detector has been verified on orbit by a previous mission. The camera system is also designed to observe dark asteroids. DELPHINUS can observe 12.0-Vmag objects with 15-seconds exposure time.

Because the duration of flashes is only 0.01 seconds to 0.1 seconds, a 60-fps (frame per second) camera system is needed. However, the camera system generates huge image data, and EQUULEUS cannot downlink all data to the ground due to the limitation of communication capacity. Therefore, real-time and on-board LIF detection algorithm is essential, and the algorithm is implemented on the FPGA based processing board. The key point of the design of LIF detection algorithm is how to correctly detect transient LIFs from the huge data with large noises. To distinguish a true LIF from noise, the algorithm uses point spread function (PSF) information of LIFs, which is completely different from a systematic noise. In addition, for more robust determination of LIFs, DELPHINUS has two cameras and extracts two LIF candidate images from both cameras at the same timing. These two images will be

downlinked and verified whether both images have similar flashes by science operator. The detail of the automatic LIF detection algorithm is described in Ref. 23.

Table 3: Specifications of DELPHINUS

Content	Value
Mass and size of telescope	0.57kg / 100 × 100 × 50mm
Mass and size of circuit board	0.07 kg / 100 × 100 mm
Power	4.0 W (maximum)
Pixel number and size	659 × 494 / 7.4 × 7.4 μm
Wavelength	400 nm – 800 nm
Lens	f = 500 mm, F1.4
Frame Rate	60 fps (maximum)
Detectable magnitude	4.5 Vmag (S/N=2) with 1/60 sec exposure time

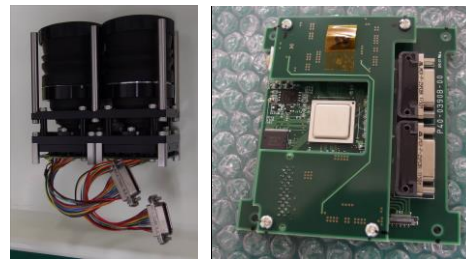


Figure 8: Flight model of DELPHINUS (left: Telescope, right: Circuit board)

Development Status

The flight model of the two cameras and the FPGA based image processing board was completely developed, and several optical tests were conducted. The dark noise property depends on detector temperature was measured in a thermal cycle test. The focal length and PSF were verified in a unit thermal vacuum test. The sensitivity and flatness property of the optical system were measured by using a well calibrated integrating sphere. The limiting magnitude was estimated from data obtained in a real-sky test. Finally, a unit vibration test was conducted, and after that, it was verified that the optical properties were not changed by the vibration.

The real-time and on-board LIF detection algorithm was also developed and implemented on the FPGA board. The algorithm was verified by using a hardware based LIF simulator newly developed for DELPHINUS. Figure 9 shows the hardware optics simulator (right) and the flight model of DELPHINUS (left). The hardware simulator is constructed by a laser diode, a pulse generator, a dark filter, a collimator, and a beam splitter. A light generated by the laser diode is controlled by the pulse generator to emulate the

momentum LIF phenomena. The dark filter tunes the magnitude of the light to suit a required magnitude of a LIF. The collimator converts the light to parallel light, and the beam splitter splits the parallel light to input the emulated LIF into both cameras of DELPHINUS.

The LIF detection algorithm test was successfully demonstrated by using the hardware simulator. The simulator generated 4.0 Vmag LIFs, and DELPHINUS successfully detected the LIFs with both cameras even though the split beams were not completely aligned, and the position of the LIFs were not the same in the two cameras. The algorithm can calibrate such kinds of mis-alignments between two cameras, and it was also demonstrated in the test. Figure 10 shows a result of the hardware test. In the LIF detection algorithm, 4 images are extracted and stored from each camera (totally 8 images): an image at the LIF detection timing, an image before the detection, and two images after the detection. By using the before and after images, we can see the time variation of the magnitude of flashes. It is also robust for the timing offset between two cameras because the two cameras are not synchronized, and a frame offset may happen. A noise tolerance test was also executed in the thermal cycle test. During the thermal cycle test, the LIF detection algorithm was activated long time without any light incidence. The threshold to detect LIFs was set to a corresponding value with 4.0 Vmag, and it was verified that overloaded mis-detections did not occur.

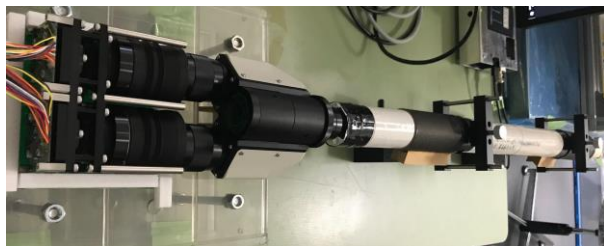


Figure 9: Hardware LIF simulator

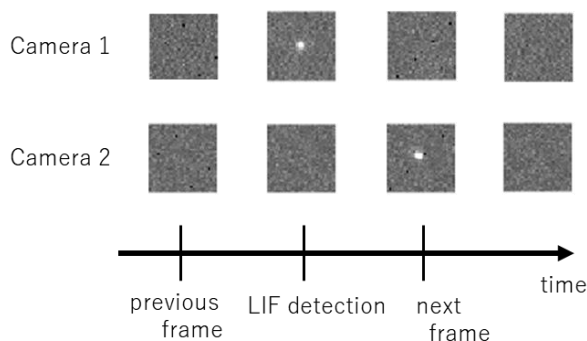
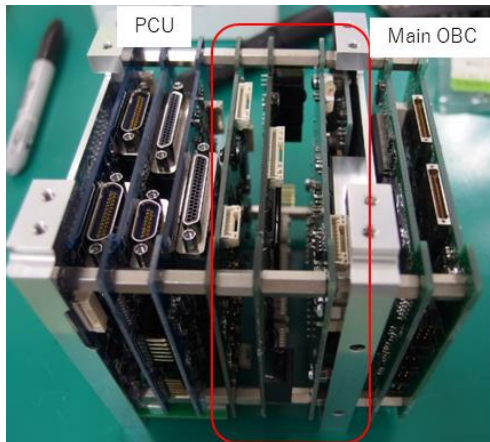


Figure 10: A result of hardware test (1.0 Vmag LIF)

INTEGRATION AND TESTING

The developments and unit tests of the flight models of the three science instruments have been completed, and we started flight model integration and testing of EQUULEUS spacecraft. The flight model of EQUULEUS was integrated at the clean room in the University of Tokyo by students. Figure 11 shows the integrated circuit board box of 1U size. The box includes the main OBC, the PCU (Power Control Unit), and three circuit boards for the science instruments explained above. Figure 12 shows the integrated flight model of EQUULEUS. You can see the smart MLI of CLOTH, the two telescopes of DELPHINUS with cover (non-flight item), and the telescope of PHOENIX. The telescopes of DELPHINUS and PHOENIX are housed within the 1U size.

After the integration was finished, integrated tests were conducted. By the June 2019, an all function test, an integrated thermal cycle test, and a thermal vacuum test were completed. In the function test, hardware level connection and software level communication among all components and all functions of each component were tested in the integrated configuration including a communication with a ground station. Mutual interference among components was also tested. In the thermal cycle test, the flight model was installed in -20 to 50 degrees environment and tested most of the functions. In the thermal vacuum test, the flight model was installed into a thermal vacuum chamber and also tested the functions in a vacuum environment. In addition, the data related with thermal model was obtained to calibrate thermal parameters to suit real spacecraft configuration. Through the integrated tests, we found several small problems, and they can be fixed by the shipment deadline. After the modification of the small problems, we will conduct the final vibration test for the flight model of EQUULEUS. We also will complete the development of flight software, and send it to the KSC for the launch of SLS-EM1.



Circuit Boards of Science Payloads

Figure 11: Integrated circuit boards

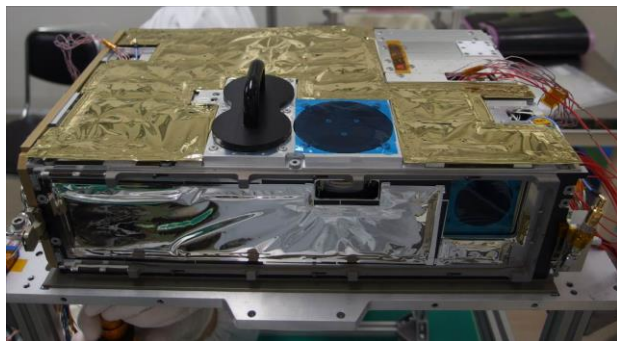


Figure 12: Flight model of EQUULEUS w/o SAP

CONCLUSIONS

This paper summarized the science objectives, design results, and current development status of the three science instruments installed in EQUULEUS spacecraft. PHOENIX: an extreme ultraviolet telescope observes the plasmasphere around the earth to clarify the physical process governing the terrestrial plasmas and improve our understanding of the radiation environment around the earth. CLOTH: a dust detector integrated with thermal blanket observes micrometeoroids environment in the cislunar region to provide the first insight of spatial distribution of sub-mm solid objects in the region. DELPHINUS: a lunar impact flash telescope observes transient flashes generated by an impact of meteoroids on the moon surface to investigate size distribution, influx ratio and daily variation of meteoroids around the cislunar region.

These instruments were designed and developed to satisfy the requirements derived from the science objectives under the constraints derived from the spacecraft configurations. The performance and space

environment tolerance of the developed flight models were verified by unit test. Several problems found in the previous proto type models were already fixed.

The full flight model integration was also completed, and function tests and environment tests were conducted. These tests were almost successful, but several small problems to modify by the launch were revealed. We will modify the small problems, develop flight software, and conduct final vibration test by the shipment deadline to launch by the SLS-EM1 rocket.

Acknowledgments

We would like to thank all students and staffs in the EQUULEUS team, who are working hard for the success of the spacecraft mission. We also would like to thank MEISEI ELECTRIC CO. LTD. for the contribution to the development of PHOENIX and COSINA CO. LTD., Imagetech CO. LTD., and WATEC CO. LTD for the contribution to the development of DELPHINUS.

References

1. R. Funase, T. Inamori, S. Ikari, and *et al.*, "One-year Deep Space Flight Result of the World's First Full-scale 50kgclass Deep Space Probe PROCYON and Its Future Perspective", 30th Annual AIAA/USU Conference on Small Satellite, Utah, USA, 2016.
2. Y. Shinnaka, N. Fougere, H. Kawakita, and *et al.*, "Imaging observations of the hydrogen coma of comet 67P/Churyumov-Gerasimenko in September 2015 by the PROCYON/LAICA", *The Astronomical Journal*, Vol.153, No.2, pp.76-81, 2017.
3. S. Kameda, S. Ikezawa, M. Sato, and *et al.*, "Ecliptic north-south symmetry of hydrogen geocorona", *Geophysical Research Letters*, Vol.44, Issue 23, 2017.
4. A. Klesh, B. Clement, C. Colley, and *et al.*, "MarCO: Early Operations of the First CubeSats to Mars", 32nd Annual AIAA/USU Conference on Small Satellite, Utah, USA, 2018.
5. R. Funase, S. Ikari, Y. Kawabata, and *et al.*, "Flight Model Design and Development Status of the Earth—Moon Lagrange Point Exploration CubeSat EQUULEUS Onboard SLS EM-1", 32nd Annual AIAA/USU Conference on Small Satellite, Utah, USA, 2018.
6. Y. Kawabata, K. Kakihara, N. Berasi, and *et al.*, "Navigation analysis for Launch and Early Operation Phase: EQUULEUS", *Proceedings on 32nd ISTS*, Fukui, Japan, 2019

7. D. Mori, A. Ishikawa, H. Seki, and R. Funase, "Structural Design of Lunar CubeSat EQUULEUS and Lessons Learned for Future Missions", Proceedings on 32nd ISTS, Fukui, Japan, 2019
8. S. Nomura, R. Takahashi, K. Tomita, and *et al.*, "Updates on EQUULEUS ADCS: Design of the Critical "DV1" Operation and Initial Results from Hardware-In-the-Loop Simulations", Proceedings on 32nd ISTS, Fukui, Japan, 2019
9. Y. Murata, N. Funabiki, H. Aohama, and *et al.*, "Power Management of Lunar CubeSat Mission EQUULEUS Under Uncertainties of Power Generation and Consumption", Proceedings on 32nd ISTS, Fukui, Japan, 2019
10. K. Nishii, J. Asakawa, A. Hattori, and *et al.*, "Flight Model Development of a Water Resistojet Propulsion System: AQUARIUS Installed on a 6U CubeSat: EQUULEUS", Proceedings on 32nd ISTS, Fukui, Japan, 2019
11. T. Shibukawa, S. Matsushita, K. Iiyama, and R. Funase, "Implementation and Verification of the Tightly-Coupled Thermal Design of the 6U Deep Space CubeSat EQUULEUS", Proceedings on 32nd ISTS, Fukui, Japan, 2019
12. I. Yoshikawa, A. Yamazaki, G. Murakami and *et al.*, "Telescope of extreme ultraviolet (TEX) onboard SELENE: science from the Moon", Earth, Planets and Space, Vol.60, Issue 4, pp.407-416, 2008.
13. I. Yoshikawa, T. Homma, K. Sakai, and *et al.*, "Imaging observation of the Earth's plasmasphere and ionosphere by EUVI of ISS-IMAP on the International Space Station", IEEE Transactions on Fundamentals and Materials, Vol.131, No.12, pp.1006-1010, 2011.
14. K. Yoshioka, G. Murakami, A. Yamazaki *et al.*, "The extreme ultraviolet spectroscopy for planetary science, EXCEED", Planetary and Space Science, Vol.85, pp.250-260, 2013.
15. T. Hirai, M.J. Cole, and *et al.*, "Microparticle Impact Calibration of the Arrayed Large-AreaDust Detectors in INterplanetary Space (ALADDIN) Onboard the Solar Power Sail Demonstrator IKAROS", Planetary and Space Science, Vol.100, pp.87-97, 2014.
16. T. Hirai, H. Yano, and *et al.*, "Data Screening and Reduction in Interplanetary Dust Measurement by IKAROS-ALADDIN", Advances in Space Research, Vol.59, Issue 6, pp.1450-1459, 2017.
17. T. Hirai and H. Yano, "MULTI-LAYER INSULATION, SPACECRAFT, DAMAGE DIAGNOSIS DEVICE, AND METHOD OF DETECTING OBJECT TO BE DETECTED", December 22, 2017, Japan Patent JP2017-246925.
18. N. Kawai, K. Tsurui, S. Hasegawa and E. Sato, "Single microparticle launching method using two-stage light-gas gun for simulating hypervelocity impacts of micrometeoroids and space debris", Review of Scientific Instruments, 81 (2010), pp. 115105.
19. R. Jitsukawa, H. Yano, T. Hirai, and *et al.*, " COMPUTATIONAL AND EXPERIMENTAL PREDICTION FOR COSMIC DUST DETECTION BY THE EQUULEUS-CLOTH SYSTEM IN THE EARTH- LUNAR LAGRANGIAN 2 REGION", Advances in Space Research, in submit.
20. L. Mohon, "Lunar Impacts", NASA, https://www.nasa.gov/centers/marshall/news/lunar/lunar_impacts.html
21. R. Fuse, S. Abe, M. Yanagisawa, R. Funase, and H. Yano, "Space-based Observation of Lunar Impact Flashes", Transactions of the Japan Society for Aeronautical and Space Sciences, Aerospace Technology Japan, Vol.17, pp. 315-320, 2019.
22. A.M. Cipriano, D.A. Dei Tos, and F. Topputo, "Orbit design for LUMIO: The lunar meteoroid impacts observer", Frontiers in Astronomy and Space sciences, 5 2018, pp. 1-23
23. M. Fujiwara, S. Ikari, H. Kondo, and *et al.*, "Development of On-board Image Processing Algorithm to Detect Lunar Impact Flashes for DELPHINUS", Proceedings on 32nd ISTS, Fukui, Japan, 2019